Chaotic bursting at the onset of unstable dimension variability

Ricardo L. Viana,[1] Sandro E. de S. Pinto,[1] and Celso Grebogi[2]
[1]*Departamento de Física, Universidade Federal do Paraná, Caixa Postal 19081, 81531-990 Curitiba, Paraná, Brazil*
[2]*Instituto de Física, Universidade de São Paulo, Caixa Postal 66318, 05315-970 São Paulo, São Paulo, Brazil*
(Received 5 June 2002; published 21 October 2002)

Dynamical systems possessing symmetries have invariant manifolds. According to the transversal stability properties of this invariant manifold, nearby trajectories may spend long stretches of time in its vicinity before being repelled from it as a chaotic burst, after which the trajectories return to their original laminar behavior. The onset of chaotic bursting is determined by the loss of transversal stability of low-period periodic orbits embedded in the invariant manifold, in such a way that the shadowability of chaotic orbits is broken due to unstable dimension variability, characterized by finite-time Lyapunov exponents fluctuating about zero. We use a two-dimensional map with an invariant subspace to estimate shadowing distances and times from the statistical properties of the bursts in the transversal direction. A stochastic model (biased random walk with reflecting barrier) is used to relate the shadowability properties to the distribution of the finite-time Lyapunov exponents.

DOI: 10.1103/PhysRevE.66.046213 PACS number(s): 05.45.Ac, 05.45.Pq

I. INTRODUCTION

When a chaotic dynamical system has some phase-space symmetry it may exhibit an invariant manifold in which lies its chaotic invariant set, with the corresponding transversal manifold [1]. A physically relevant example is the particle motion under a central force, whose intensity depends only on the absolute value of the distance between the particle and the center of force. The spherical symmetry constrains the particle trajectories to lie on a plane [2]. The dynamics is thus confined to a four-dimensional invariant subspace embedded in the full six-dimensional phase space of the system. Any dependence of the force on the spherical angles would break the spherical symmetry and the phase-space trajectories would no longer be constrained to live in this subspace. Another example is an assembly of coupled identical chaotic oscillators, say, of Rössler systems [3]. If the coupling constants satisfy a given mathematical condition, it may be shown that a low-dimensional synchronization manifold exists for which all chaotic oscillators are in phase [4,5]. If the synchronization manifold is not transversely stable, however, typical trajectories never asymptote to it.

The synchronization of a coupled chaotic system depends on the transversal stability properties of the invariant manifold (when it exists) in the phase space [3,6,7]. To analyze the loss of transversal stability, one must consider those unstable periodic orbits in the chaotic trajectory embedded in the invariant manifold and determine when they become transversely unstable [8]. A master stability function technique was proposed to implement this procedure for coupled chaotic discrete and continuous-time systems [9].

In this paper, we investigate the behavior of chaotic trajectories off but close to the invariant manifold in a chaotic system possessing an invariant subspace. Under certain conditions these trajectories have an almost regular transversal dynamics, characterized by laminar behavior interrupted by chaotic bursts in an intermittent fashion. This situation has been extensively studied as a form of *on-off intermittency*, when there is an invariant manifold [10], and as *in-out intermittency*, when there is not [11]. On-off intermittency is distinguished by its universal scaling for the average duration of the laminar region, and has been observed also in experiments [12].

The main point of this paper is that shadowability breakdown for chaotic trajectories in the invariant manifold is an important consequence of the loss of transversal stability associated with chaotic bursting. A chaotic true trajectory is said to be *continuously shadowable* if there exists another chaotic trajectory which: (i) stays close to the former one for a sufficiently long time, and (ii) may be continuously deformable to the chaotic trajectory [13]. If the chaotic trajectory is continuously shadowable, there is a continuous family of noisy trajectories which are shadowed by the same fiducial chaotic trajectory of the system. For calculating long-time averages of quantities such as entropies and dimensions it does not matter which noisy trajectory one would take, provided that this noisy trajectory can be continuously deformed into the true trajectory.

It turns out, however, that shadowability is not a mathematical property which can always be taken for granted in chaotic systems. It has been proved that shadowability only holds for an infinite time for the special case of hyperbolic systems [14–16], and the majority of dynamical systems, likely to be found in physical applications, are nonhyperbolic. Hyperbolic systems have the splitting between unstable and stable directions continuously valid for all points on the invariant set, and the angle between the corresponding manifolds is bounded away from zero. When the latter condition is violated by homoclinic tangencies, shadowability is still valid for a finite time span [19,17,18].

We will focus on another and stronger form of shadowability breakdown, caused by the violation of the continuous splitting of stable and unstable directions in the invariant set. This occurs when the unstable periodic orbits embedded in the chaotic invariant set have different number of unstable directions, and has been called unstable dimension variability (UDV). UDV was first described in the mathematical literature in the early 1970's [20], but its existence in chaotic systems of physical interest was first reported (for the periodically kicked double rotor) more than two decades later

 ©2002 The American Physical Society

[21,22]. It was also observed that a hallmark of UDV is the fluctuating behavior (about zero) of the finite-time Lyapunov exponent closest to zero. A very drastic consequence of UDV is the almost complete breakdown of shadowability for typical chaotic trajectories, in the sense that no actual chaotic trajectory is continuously shadowed by a computer-generated (noisy) chaotic orbit [23,24]. Moreover, microscopic one-step errors inherent to the numerical algorithms used to obtain a trajectory may cause macroscopic errors, many orders of magnitude larger, in long-term averages [25]. Hence computer-simulated long-time statistics of chaotic dynamical systems exhibiting UDV may not yield useful information, even though being correctly obtained from physical laws, and can more properly be quoted as *pseudodeterministic systems* [6].

This paper investigates the connection between chaotic bursting and the breakdown of shadowability via UDV for a two-dimensional map with an invariant subspace. We describe the existence of intermittent chaotic bursting for this system by studying the spike heights in the transversal direction as the pointwise shadowing distances. In the same spirit, the shadowing time is taken as the duration of the laminar regions between two consecutive chaotic bursts, when the shadowing distance is of the order of unity. Our numerical results are then compared with a stochastic model which assumes a biased random walk with reflecting barrier [26], in such a way that the shadowing distances and times are related to the statistical properties of the finite-time Lyapunov exponents in the transversal direction.

Our results support the following conjectures: (i) chaotic bursting appears at the onset of UDV in chaotic systems with an invariant subspace and with a number of transversely unstable periodic orbits; (ii) the shadowability of chaotic trajectories is worse as the UDV effect is more intense. In particular, when the latter is maximum, the shadowing time—as we define—vanishes. Although we have used a simple discrete-time system to draw these conclusions, we claim that they can be applicable, for example, to higher-dimensional coupled chaotic systems.

The rest of this paper is organized as follows: in Sec. II we introduce the two-dimensional map with invariant subspace used to study the relation between bursting and UDV; in Sec. III we present numerical results for shadowing distances and times in this model. Section IV quantifies the nonhyperbolicity via UDV by means of finite-time Lyapunov exponents in the direction transverse to the invariant subspace; and the properties of these exponents are used in Sec. V to derive a stochastic model (biased random walk with reflecting barrier) which will be used to explain the numerical results obtained. The last section contains our conclusions.

II. CHAOTIC BURSTING IN A SYMMETRIC SYSTEM

We consider a class of two-dimensional noninvertible maps with a skew-product structure and having the dynamical properties we wish to study,

$$x_{n+1}=f(x_n), \tag{1}$$

$$y_{n+1}=pg(x_n)y_n+\text{higher-order odd powers of } y_n, \tag{2}$$

where $x\in J\subseteq R^1$ and $y\in R^1$. Due to the reflection ($y\to -y$) symmetry there is an invariant subspace $\mathcal{M}$ given by $y=0$, with y as the corresponding transversal direction. The map (1) is such that there is a chaotic invariant set $\Omega\subset\mathcal{M}$, and $p>0$ is a bifurcation parameter, such that: (i) $pg(x_n)\geqslant 0$ for all $x\in J$; and (ii) $g(x)=1$, when $x=\chi$ is some unstable periodic orbit embedded in Ω.

An example of this class of systems is [27]

$$x_{n+1}=ax_n(1-x_n), \tag{3}$$

$$y_{n+1}=pe^{-b(x_n-\chi)^2}y_n-y_n^3, \tag{4}$$

where $J=[0,1]$, and we choose the parameter a so that there is a dense chaotic orbit in Ω. For the logistic map (3) there is a positive Lebesgue measure set of values of a for which this is true [28]; and we adopt $a=4$, so that the invariant set is $\Omega=J$, in such a way that $\chi=1-(1/a)=3/4$ is the unstable fixed point belonging to Ω. This is the first periodic orbit of Ω to lose transversal stability, as the bifurcation parameter p is varied. If $p<1$, it is a transversely stable saddle with unstable dimension 1 (the x direction is unstable) [27]. An unstable-unstable pair bifurcation (with eigenvalue $+1$) occurs at $p=p_c=1$, after which the fixed point at $x=\chi$ becomes a transversely unstable repeller with unstable dimension 2. This bifurcation also signals a boundary crisis, for the newborn repeller coalesces with two other repellers belonging to the basin boundary of the chaotic attractor in $\mathcal{M}$ [7]. Hence, the chaotic invariant set Ω, which is an attractor for $p<p_c$, becomes a nonattracting chaotic saddle for $p\geqslant p_c$ [29].

When the fixed point at $x=\chi$ loses transversal stability, every preimage also does it. As there is a denumerable infinite and dense set of such eventually fixed points embedded in the chaotic set [30], it turns out that a dense set of saddles become repellers. As a result of the saddle-repeller bifurcation, the repeller and the saddle sets are densely intertwined in J. The saddle-repeller bifurcation marks the onset of UDV in the system. The transversal dynamics after the bifurcation is the result of a competition between attracting and repelling tendencies, as a trajectory off the invariant subspace visits the neighborhood of a saddle or repeller, respectively. Anchored at each repeller there is a tonguelike structure projecting itself over positive and negative values of y due to the nonlinear term in Eq. (4) (see Fig. 1) [27,7]. An orbit entering in such tongue will be rapidly repelled from the invariant subspace. Since these tongues are dense and typically supernarrow near $\mathcal{M}$, it takes a very long time for a given orbit to enter them (superpersistent chaotic transients) [31]. The complement of the tongues is a Cantor-like set of positive Lebesgue measure, or a fat fractal [32]. The orbit returns to a vicinity of the invariant subspace along this set.

This is the basic mechanism of the chaotic bursting observed for trajectories off but very close to the invariant subspace . An initial condition $y_0\approx 0$ will generate a trajectory that wanders back and forth in the x direction, approaching an infinite number of intertwined saddles and repellers em-

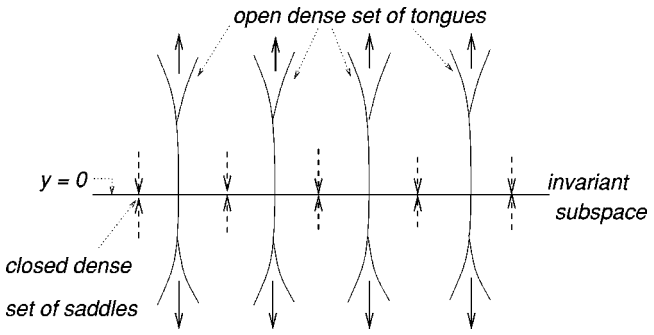

FIG. 1. Schematic representation of the unstable periodic orbit structure appearing after a saddle-repeller bifurcation. Adapted from Ref. [27].

bedded in $\mathcal{M}$. If p is not much larger than the bifurcation point $p_c=1$, there is a predominance of saddles, and the orbit is kept in the vicinity of the invariant subspace, so generating the laminar regions in the transversal dynamics. Once an orbit approaches a tongue, the resulting escape and reinjection leads to a chaotic burst, followed by another laminar regime and so on. As p is further increased, other unstable periodic orbits embedded in the chaotic set Ω will lose transversal stability, and more and more saddles become repellers. The relative proportion between saddles and repellers will change with increasing p, and this will reflect in the average duration of the laminar regions, since as the relative repeller population increases in Ω, chaotic bursting becomes more frequent.

The relative dominance of saddles and repellers in Ω can be quantitatively described by their contributions to the natural ergodic measure of the invariant chaotic set. The natural measure in Ω is computed by using a typical trajectory, since it originates from a randomly chosen initial condition [33]. However, the set of unstable periodic orbits embedded in Ω, having zero Lebesgue measure, generates atypical measures; and there is an infinite number of such atypical measures, supporting the typical natural measure on Ω. A relation between these typical and atypical measures was proven to exist for hyperbolic systems [34], but numerical evidence has been given to extend its validity to nonhyperbolic ones [35]. A typical trajectory eventually visits any neighborhood, no matter how small, of any unstable periodic orbit in Ω. Hence, there are different contributions to the natural measure from saddles and repellers, in the sense of carrying different weights to the total measure [8].

III. SHADOWING DISTANCES AND TIMES

After the saddle-repeller bifurcation at $p=p_c$ the invariant chaotic set Ω becomes nonhyperbolic (the splitting between stable and unstable directions is no longer continuous along Ω) and we expect that the shadowability of chaotic trajectories in Ω breaks down for $p \geqslant p_c$. In this spirit, we can call the process UDV *intermittency*, since here chaotic bursting is accompanied by the lack of hyperbolicity (in Ref. [25] UDV is also called an ''intermittency in miniature'').

In order to describe how shadowing distances and times are numerically estimated, we consider a reference, or ''true'' chaotic trajectory in $\Omega \subset \mathcal{M}$. However, the existence of the invariant subspace $\mathcal{M}$ is jeopardized by the lack of model symmetry caused by small, yet unavoidable, imperfect parameter determination, and extrinsic noise. We thus expect that a computer-generated trajectory will start off but very close to $\mathcal{M}$. The shadowing distance between the ''true'' chaotic trajectory at $\mathcal{M}$ and the pseudotrajectory initialized nearby is, at each instant, the pointwise distance between them in the phase plane. The existence of laminar intervals, for which the pseudotrajectory is close to $\mathcal{M}$, is equivalent to having a pseudotrajectory that continuously shadows the ''true'' chaotic trajectory belonging to $\mathcal{M}$. By the same token, bursting is an observable manifestation for the lack of shadowability, while the lengths of the laminar intervals yield estimates for the shadowing times. Hence, the properties of chaotic bursting are related to the statistics of shadowing distances and times.

We present numerical results for the map (3),(4), considering fixed values of a and b, and varying the bifurcation parameter $p>1$ to achieve situations where UDV and chaotic bursting occur. A ''true'' chaotic trajectory is known to exist for initial trajectories $(x,y=0)$ randomly chosen in Ω with respect to the Lebesgue measure. The pseudotrajectories we generate are meant to represent numerically obtained orbits, for which we cannot have an initial condition exactly placed at $y=0$ but which, instead, will have some transversal uncertainty. Since the x part of the map (3) does not depend on y, the evolution along the x direction of both trajectories is the same for all times, and the pointwise distance between a chaotic trajectory and a pseudotrajectory will be simply the value of y_n for the latter. Finally, a computer-generated pseudotrajectory is likely to suffer the action of roundoff errors, which we can systematically simulate by corrupting our pseudotrajectory with randomly applied kicks of small magnitude 10^{-q}, which play the role of one-step errors [36].

We must emphasize that the pseudotrajectories do not belong to Ω but are, strictly speaking, bona fide chaotic trajectories belonging to a larger invariant set in which Ω is a subset. The fold introduced in the y part of the map (4) ensures that this larger chaotic set is recurrently close to $\mathcal{M}$ and does not asymptote to infinity, as it would be the case if the cubic term in Eq. (4) would have a positive sign, as in Ref. [27]. In the latter case, one would have a chaotic transient. However, our results are not essentially dependent on the existence of this fold, since if the chaotic transient would escape to infinity, we would generate other chaotic transients by choosing another initial condition close to $\mathcal{M}$. In Fig. 2, we show two examples of high-precision pseudotrajectories generated using the procedure described above. The noise level is fixed at 10^{-16}, which can be regarded as the computer roundoff introduced by a double precision floating-point arithmetics. Figures 2(a) and 2(b) refer to different postcritical values of the bifurcation parameter $(p>1)$. We record the values of y_n, or the pointwise shadowing distances, at each time, yielding the corresponding log distances $z_n=\ln|y_n|$. The use of an external kick creates a ''barrier'' of width 10^{-q} preventing pseudotrajectories from having shadowing log distances less than q on average. The shadowing

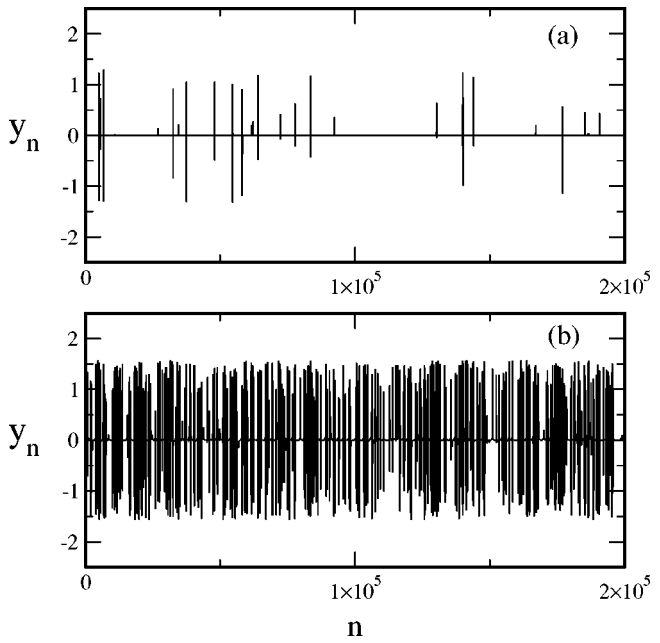

FIG. 2. Pseudotrajectories for the map (3),(4) with $a=4.0$, $b=5.0$, and a noise level 10^{-q}, with $q=16$, and (a) $p=2.30$; (b) $p=2.55$.

distances may be large due to chaotic bursting, but they are predominantly very small (within the laminar regions); the bursting being more effective as p increases.

Figure 3 presents statistical distributions of the shadowing log distances z_n for two postcritical values of p and external kicks of different magnitudes. In all depicted cases, the (normalized) distribution height falls rapidly down to zero for shadowing distances less than 10^{-q}, as expected, and decreases exponentially for higher shadowing distances

$$P_d(z)=P_{d0}\exp[-\kappa(p)(z-\ln q)], \tag{5}$$

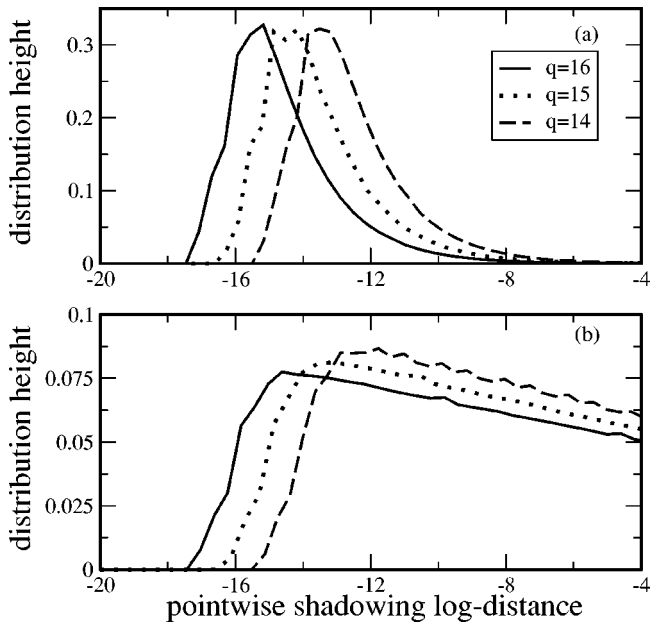

FIG. 3. Statistical distribution of pointwise shadowing log distances for (a) $p=2.10$, (b) $p=2.55$, and three different noise levels.

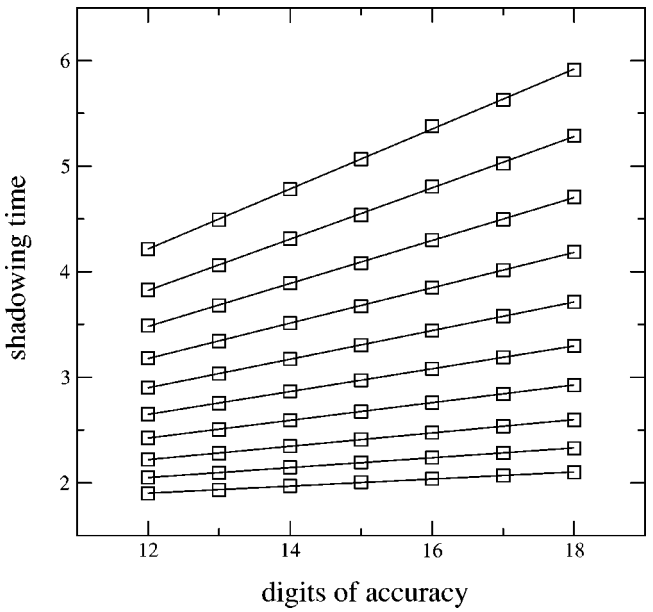

FIG. 4. Shadowing times as a function of the kick strength exponent, or the number of accuracy digits. The various lines are least-squares fits obtained for different values of the bifurcation parameter p. The top line is for $p=2.1$ and the lines below are for values of p with a constant increment of $\delta p=0.05$. The slopes of these lines are depicted as boxes in Fig. 7.

where $P_d(z)dz$ is the probability for the shadowing log distance to lie between z and $z+dz$. As p increases from 2.1 [Fig. 3(a)] to 2.55 [Fig. 3(b)] this decrease becomes slower [$\kappa(p_2)<\kappa(p_1)$ for $p_2>p_1$], meaning that, as the UDV effect is more intense, we have a progressive dominance of higher shadowing distances (or taller spikes). This is in accordance with the greater content of transversely unstable periodic orbits as p is increased from $p_c=1$ and, consequently, an increased transversely repelling behavior on average.

The shadowing log distances experience spikes of various heights, but remain in the immediate vicinity of the invariant subspace $\mathcal{M}$, until they burst chaotically and return to $\mathcal{M}$. We define the shadowing time as the interval it takes for the pointwise shadowing distance to grow to the order of the attractor size, or $y=y_A=1$. Figure 4 shows the dependence of the log-shadowing times, for different values of p, on the noisy kick strength level q. The top curve was obtained for $p_0=2.1$, and the curves below correspond to $p_j=p_0+j\,\delta p$, for $j=1,2,\ldots,9$ and $\delta p=0.05$. The results suggest that the distribution of the average shadowing times is of a power-law nature with respect to the noise level q. This can also be derived by integrating the distribution (5) for shadowing log distances, in order to obtain the probability for a shadowing distance to be greater than y_A, at a given noise level q,

$$P_t(q)\sim\exp[-\kappa(p)(\ln y_A-\ln q)]=q^{\kappa(p)}. \tag{6}$$

In the next sections, we will see that these probability distributions for the shadowing distances and times can be theoretically justified by rather general arguments, and that the

characteristic exponent κ can be predicted from the statistical properties of the finite-time Lyapunov exponents.

IV. FINITE-TIME LYAPUNOV EXPONENT

When an initial condition is placed off but near the invariant chaotic set $\Omega \subset \mathcal{M}$, it will generate an orbit that visits the neighborhood of unstable periodic orbits in Ω with different numbers of unstable directions. Now let us imagine a small ball of initial conditions having a nonempty intersection with $\mathcal{M}$. What will happen as time evolves? If the ball is placed near a saddle (transversely stable), the dynamics at a given time will make the ball shrink on average along the transversal direction and turn into a thin cigarlike tube [8]. After some time, the cigarlike tube will approach a repeller in $\mathcal{M}$ (transversely unstable) and will expand on average also along the y direction. This process is likely to repeat itself as many times as the trajectories alternately approach saddles and repellers in $\mathcal{M}$.

The finite-time Lyapunov exponents in the transversal direction, $\lambda_y(x_0,y_0,n)$, are the average rates of these temporary expansions and contractions along the y axis, for which they can be negative or positive, depending on whether the trajectory is in the neighborhood of a saddle or a repeller, respectively. They are defined, for a two-dimensional map $\mathbf{F}(x,y)$ of the form (1),(2), as [37]

$$\lambda_y(x_0,y_0=0;n)=\frac{1}{n}\ln||\mathbf{DF}^n(x_0,y_0=0)\cdot\mathbf{v}_y||, \qquad (7)$$

where $\mathbf{v}_y$ is the singular vector related to the singular value ξ_y of the n times iterated tangent map. The infinite-time limit of Eq. (7) is the transversal Lyapunov exponent

$$\lambda_T=\lim_{n\to\infty}\lambda_y(x_0,y_0=0;n), \qquad (8)$$

and has the same value for almost all $x_0 \in J$, whereas its finite-time counterpart does depend on x_0. On considering the map (3),(4) for $p>1$, the intertwined sequence of saddles and repellers in $\mathcal{M}$ is such that a bursting trajectory will have nonoverlapping sections of finite duration, for which λ_y fluctuates about zero [22].

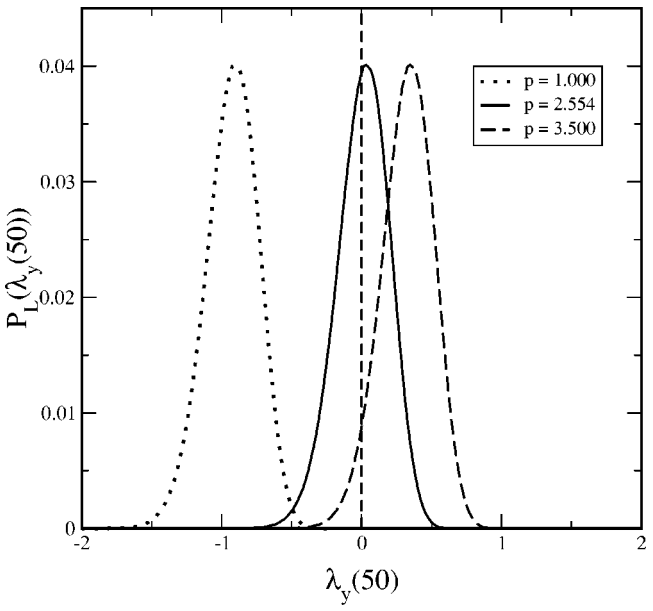

FIG. 5. Probability distributions for finite-time transversal Lyapunov exponents for $n=50$ and different values of the bifurcation parameter.

It is useful to introduce another probability distribution $P_L(\lambda_y(x_0,y_0;n),n)$ for the finite-time Lyapunov exponents, where the initial conditions $(x_0,y_0=0)$ are randomly chosen according to the Lebesgue measure of Ω. From this probability distribution, we can obtain moments of functions of the finite-time exponent, as averages [37],

$$m=\langle\lambda_y(x_0,y_0=0,n)\rangle=\int_{-\infty}^{+\infty}\lambda_y(x_0,y_0=0,n)P_L(\lambda_y(x_0,y_0=0,n),n)d\lambda_y, \qquad (9)$$

and dispersions,

$$\sigma_n^2=\langle[\lambda_y(x_0,y_0=0,n)-m]^2\rangle=\langle\lambda_y^2\rangle-\langle\lambda_y\rangle^2, \qquad (10)$$

assuming proper normalization for $P_L(\lambda_y)$.

For n large enough, this distribution can be written in the following form [38]:

$$P_L(\lambda_y(n),n)\approx\sqrt{\frac{nG''(\lambda_T)}{2\pi}}e^{-nG(\lambda_y)}, \qquad (11)$$

where the function $G(\lambda_y)$ is such that $G(\lambda_T)=G'(\lambda_T)=0$ and $G''(\lambda_T)>0$. Expanding in powers of $\lambda_y-\lambda_T$, we have a Gaussian probability distribution,

$$P_L(\lambda_y(n),n)\approx\sqrt{\frac{nG''(\lambda_T)}{2\pi}}\exp\left[-\frac{nG''(\lambda_T)}{2}(\lambda_y-\lambda_T)^2\right]. \qquad (12)$$

We can obtain a numerical approximation for this probability distribution by considering a large number of trajectories of fixed length, say $n=50$, from initial conditions randomly chosen in Ω. Figure 5 shows the distribution of the finite-time exponents, $P(\lambda_y(50))$, for three different values of the bifurcation parameter p. The distributions have a Gaussian-like shape, as expected from Eq. (12), and the distribution as a whole drifts toward positive values of λ_y, as p increases, without noticeable distortion. This is illustrated by

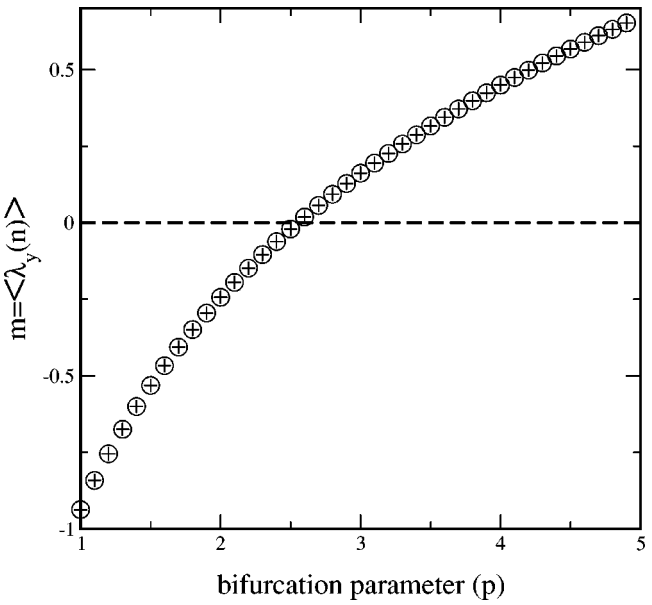

FIG. 6. Average value of finite-time transversal Lyapunov exponents vs the bifurcation parameter p, for $n=1$ (circles) and $n=50$ (crosses).

Fig. 6, where we depict the average finite-time exponent (9) versus p, showing that m builds up toward positive values as p increases, and vanishes at $p=p^*\approx 2.55$. Note that the plot does not change if we use time delays widely different from each other (like $n=1$ and $n=50$). In fact, it follows, from Eq. (12), that the average finite-time exponent does not depend on n and it is equal to the infinite-time exponent $m=\lambda_T$, given by Eq. (8), and which governs the transversal stability of Ω as a whole. The point $p^*=2.55$ is known as a *blowout bifurcation*, since Ω becomes transversely unstable for $p>p^*$ [8]. In this situation, the saddles and repellers of Ω carry equal weights in their relative contributions to λ_T, in terms of the natural measure of Ω, so that their contributions are precisely balanced at $p=p^*$.

The dispersion, or variance of the average m with respect to a sample of size n, given by Eq. (10), is constant for all p values. This means that the probability distribution does not alter its shape as p changes (see Fig. 5). Using Eq. (12) we find, for a Gaussian distribution, that $\sigma_n^2=1/G''(\lambda_T)$ does not depend on n. However, for later reference, we note that the variance of the total population is equal to the product of the variance of the average by the sample size [39], such that the total variance of the finite-time exponents is $\sigma^2=n\sigma_n^2$.

V. A STOCHASTIC MODEL FOR SHADOWING DISTANCES

The link between shadowability breakdown and chaotic bursting is the mixing between unstable orbits with different numbers of unstable directions, and this diversity should be reflected in the statistical properties of the corresponding finite-time Lyapunov exponents. This is the main idea underlying a stochastic modeling of the chaotic bursting.

A pseudotrajectory starting off but near the invariant subspace will wander along the x direction according to the unstable eigenvalue of the periodic orbits embedded in Ω. As the trajectory approaches orbits with different numbers of unstable directions, it will move either toward or apart from Ω for finite time segments. Let y_k be the transversal distance of the pseudotrajectory at time k. During a short time interval of length n, the local expansion rate is the corresponding finite-time transversal exponent, such that $y_{k+n}\sim y_k\exp[n\lambda_y(n)]$. It follows that the log-shadowing distances satisfy $z_{k+n}\sim z_k+n\lambda_y(n)$.

When Ω exhibits UDV, at least one of the time-n exponents $\lambda_y(n)$ fluctuates in a stochastic fashion about zero, and these are the random innovations which kick the log-shadowing distances toward or away from a chaotic trajectory confined to the invariant subspace $\mathcal{M}$. Hence, the time evolution of the log-shadowing distances can be regarded as an additive random process, with a diffusion rate being given by the dispersion of the finite-time exponents, which we have measured by the total variance σ^2 of their statistical distribution $P_L(\lambda_y(n),n)$. However, the distribution of $\lambda_y(n)$ is such that there is a different amount of positive and negative values (see Fig. 5). For example, if their average m is positive the transversal displacements of a pseudotrajectory will have a positive average expansion rate, which describes a biased random walk, in which a drift m has been included [26]. The arguments above justify the use of a Chapman-Kolmogorov diffusion equation for the spatiotemporal evolution of the distribution of the shadowing log distances $\mathcal{P}(z,n)$ with respect to the time n and the log distance z (assumed to be continuous variables) [40],

$$\frac{\partial\mathcal{P}(z,n)}{\partial t}=\frac{\sigma^2}{2}\frac{\partial^2\mathcal{P}(z,n)}{\partial z^2}+m\frac{\partial\mathcal{P}(z,n)}{\partial z}. \tag{13}$$

We have obtained a chaotic pseudotrajectory by: (i) placing the initial condition off but close to the invariant subspace; and (ii) adding kicks of a constant strength 10^{-q} to it. The latter feature can be included in a stochastic model of the situation by a reflecting barrier placed on $y^*=10^{-q}$, which implies a boundary condition at $z^*\simeq q$. Moreover, we have to impose the following boundary conditions: $\mathcal{P}(z\to\infty)=(\partial\mathcal{P}/\partial z)_{z\to\infty}=0$. The diffusion process governed by Eq. (13) has an equilibrium distribution given by $(\partial\mathcal{P}_{EQ}/\partial n)=0$, which reads

$$\mathcal{P}_{EQ}(z,n)=\frac{2|m|}{\sigma^2}\exp\left[-\frac{2|m|}{\sigma^2}(z-\ln q)\right], \tag{14}$$

which is similar to the numerically obtained distribution $P_d(z)$, given by Eq. (5), provided we identify the decay exponent κ with the so-called *hyperbolicity exponent* [25],

$$h\equiv\frac{2|m|}{\sigma^2}. \tag{15}$$

The statistical distributions in Fig. 3 are in fact of an exponential nature and have a cutoff at the reflecting barrier. Figure 7 shows a comparison between the numerically obtained slope of the exponentially decaying distribution (crosses) and

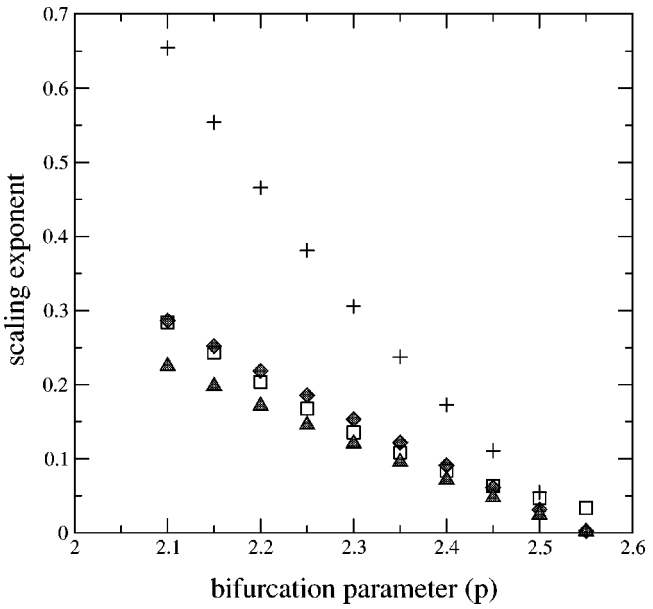

FIG. 7. Comparison between the slopes of statistical distributions of shadowing distances and times. The numerically obtained slopes for distributions of log-shadowing distances (crosses) are based on Fig. 3; diamonds (triangles) stand for the theoretical prediction of Eq. (14) based on $n=2$ ($n=50$) finite-time Lyapunov exponents; boxes are for numerically obtained distribution slopes of shadowing times, according to Fig. 4.

the theoretical prediction of Eq. (15) (diamonds and triangles are for different finite-time exponents). There is an increasingly better agreement among these values, as we approach $p=p^*=2.55$, the value for which the UDV effect is the most pronounced.

The good agreement between theory and numerical experiment at $p=p^*$ is a consequence of the fact that, when the UDV effect is more pronounced, the average finite-time exponent vanishes ($m=0$), so that there is an approximately equal number of positive and negative innovations acting on a pseudotrajectory shadowing a chaotic trajectory in Ω. In this case, the Markovian random walk approximation is very good and, as we move away from this value, the bias caused by a nonzero average exponent makes the equilibrium distribution given by Eq. (14) a poorer version of the stochastic process. Actually the bursting is chaotic, and some degree of dynamical correlation is expected to take place at every moment, preventing us from successfully using linear stochastic models such as those considered here. The finite-time exponents with $n=2$ (diamonds in Fig. 7) are consistently better than the ones with $n=50$ (shown in Fig. 7 as triangles), which implies that the underlying dynamical structure causing UDV is actually very complicated. The saddles and repellers belonging to Ω are so densely intertwined that a pseudotrajectory will suffer influences of the different number of their unstable directions over very short periods of time, and a $n=2$ exponent is expected to give results closer to a Markovian stochastic process, when compared with a $n=50$ exponent.

The stochastic model we use for a biased random walk with reflecting barrier can also be worked out to estimate the shadowing time τ, by imposing that $y_{n+\tau}$ be greater than $y_A=1$. Using Laplace transforms, we obtain the following theoretical estimate of the average shadowing time [26]:

$$\langle \tau \rangle = \frac{1}{h}(q^h-1) - \frac{\ln q}{|m|}. \tag{16}$$

In terms of the intermittent chaotic bursting, a numerical estimate for the shadowing time is the average value $\langle \tau \rangle$ of the interspike intervals, or laminar regions, yielding a statistical distribution $\tilde{P}_T$, scaling linearly with τ. For q small enough, this expression reduces to a power-law scaling with the noise level q,

$$\tilde{P}_T(q) \sim q^h, \tag{17}$$

in agreement with the numerical result of Eq. (6), provided $\kappa(p)=h$.

It should be remarked, however, that Eq. (16) may not hold if m is near zero, which nevertheless, does not spoil the small-q scaling above. This power-law scaling is confirmed by our numerical experiments. The slopes of the various curves in Fig. 4, corresponding to different values of the bifurcation parameter p, are depicted as boxes in Fig. 7. We have a better agreement between theoretical and numerical results for the shadowing time distribution than for the log-shadowing distance distribution. The reason for this fact lies in the different definitions we use for shadowing distances and times. The former are very precisely defined as pointwise distances between two trajectories, whereas the latter are defined in a less accurate way since: (i) shadowing times are measured when the log-shadowing distances exceed an arbitrary threshold; (ii) we compute average values over very long chaotic transients. Hence, the overall behavior of shadowing times is more likely emulated by a stochastic model.

VI. CONCLUSIONS

The breakdown of shadowability for chaotic trajectories due to unstable dimension variability is a very serious constraint on the applicability of mathematical models for such dynamical systems. For a physical system, even when the model is based on sound theoretical framework, there may be doubts about the validity of computer-generated trajectories, since in absence of continuous shadowability of trajectories, no pseudotrajectory of a reasonable length is expected to be shadowed by a real chaotic trajectory. Even long-time averages may be of no practical interest due to the exponential amplification of extremely small one-step errors. In this case we would have to resort to chaotic time series analysis to extract information about the system directly from the observed data. Spatially extended systems of coupled continuous or discrete time oscillators were shown to present UDV for nonzero parameter ranges, and this fact pervades an even wider class of dynamical systems, if we consider that virtually all numerical schemes for solving partial differential equations are based in some kind of discretization leading to coupled systems. In spite of this, UDV can be observed in very simple dynamical systems, like the two-

dimensional map considered in this paper.

Intermittent chaotic bursting has been extensively described in the literature, and it is present in a variety of mathematical models, as well as in experiments. When a system fails to be hyperbolic due to UDV, it may present intermittent bursting if it exhibits some symmetry leading to a low-dimensional invariant subspace. This type of intermittent transition has been observed, for example, in the transition between synchronized and non-synchronized behavior in a lattice of piecewise linear maps with a long-range coupling [41]. For general systems of N coupled maps or oscillators, the invariant subspace of interest is the M-dimensional synchronization manifold (where $M \ll N$), and we would have to investigate the corresponding $N-M$ transversal directions.

This work has focused on the relation between chaotic bursting and the nonhyperbolic structure of the invariant chaotic set embedded in the invariant subspace. Numerical evidence has been given that the distribution of the shadowing distances is of an exponential nature, the decay rate being related to the statistical properties of the finite-time Lyapunov exponents along the transversal direction. The average shadowing times, on their way, have a power-law scaling with the noise level. A theoretical stochastic model, assuming a biased random walk with reflecting barrier at the noise level, is used to explain the numerical results, and the agreement is as good as one approaches the dynamical regime where the UDV is most intense, namely, at the vicinity of a blowout bifurcation, in which the invariant subspace loses its transversal stability.

ACKNOWLEDGMENTS

This work was made possible through partial financial support from the following Brazilian and American research agencies: FAPESP, CNPq, Fundação Araucária (Paraná), and National Science Foundation. We acknowledge enlightening discussions and useful comments by S. R. Lopes and A. M. Batista.

[1] P. Ashwin, J. Buescu, and I. Stewart, Nonlinearity **9**, 703 (1996).
[2] H. Goldstein, *Classical Mechanics* (Addison-Wesley, New York, 1980).
[3] Y.-C. Lai, D. Lerner, K. Williams, and C. Grebogi, Phys. Rev. E **60**, 5445 (1999).
[4] L. M. Pecora and T. L. Carroll, Phys. Rev. Lett. **64**, 821 (1990).
[5] Y.-C. Lai and C. Grebogi, Phys. Rev. Lett. **82**, 4803 (1999).
[6] R. L. Viana and C. Grebogi, Phys. Rev. E **62**, 462 (2000).
[7] R. L. Viana and C. Grebogi, Int. J. Bifurcation Chaos Appl. Sci. Eng. **11**, 2689 (2001).
[8] Y.-C. Lai and C. Grebogi, Int. J. Bifurcation Chaos Appl. Sci. Eng. **10**, 683 (2000).
[9] L. M. Pecora and T. L. Carroll, Phys. Rev. Lett. **80**, 2109 (1998).
[10] N. Platt, E. A. Spiegel, and C. Tresser, Phys. Rev. Lett. **70**, 279 (1993); J. F. Heagy, N. Platt, and S. M. Hammel, Phys. Rev. E **49**, 1140 (1994).
[11] P. Ashwin, J. Buescu, and I. Stewart, Phys. Lett. A **193**, 126 (1994).
[12] P. W. Hammer, N. Platt, S. M. Hammel, J. F. Heagy, and B. D. Lee, Phys. Rev. Lett. **73**, 1095 (1994).
[13] C. Grebogi, L. Poon, T. Sauer, J. A. Yorke, and D. Auerbach, in *Handbook of Dynamical Systems*, edited by B. Fiedler (Elsevier, New York, 2002), p. 313.
[14] D. V. Anosov, Proc. Steklov Inst. Math. **90**, 1 (1967).
[15] R. Bowen, J. Diff. Eqns. **18**, 333 (1975).
[16] A. Katok and B. Hasselblatt, *Introduction to the Modern Theory of Dynamical Systems* (Cambridge University Press, Cambridge, 1995), Chap. 18, Sec. 1.
[17] C. Grebogi, S. Hammel, and J. A. Yorke, J. Complexity **3**, 136 (1987).
[18] C. Grebogi, S. Hammel, and J. A. Yorke, Bull. Am. Math. Soc. **19**, 465 (1988).
[19] C. Grebogi, S. Hammel, J. A. Yorke, and T. Sauer, Phys. Rev. Lett. **65**, 1527 (1990).
[20] R. Abraham and S. Smale, Proc. Symp. Pure Math. **14**, 5 (1970).
[21] F. J. Romeiras, C. Grebogi, E. Ott, and W. P. Dayawansa, Physica D **58**, 165 (1992).
[22] S. P. Dawson, C. Grebogi, T. Sauer, and J. A. Yorke, Phys. Rev. Lett. **73**, 1927 (1994).
[23] Y.-C. Lai, C. Grebogi, and J. Kurths, Phys. Rev. E **59**, 2907 (1999).
[24] S. P. Dawson, Phys. Rev. Lett. **76**, 4348 (1996); Y.-C. Lai, Phys. Rev. E **59**, R3807 (1999); E. Barreto and P. So, Phys. Rev. Lett. **85**, 2490 (2000); R. Davidchack and Y.-C. Lai, Phys. Lett. A **270**, 308 (2000).
[25] T. D. Sauer, Phys. Rev. E **65**, 036220 (2002).
[26] T. Sauer, C. Grebogi, and J. A. Yorke, Phys. Rev. Lett. **79**, 59 (1997).
[27] Y.-C. Lai, C. Grebogi, J. A. Yorke, and S. C. Venkataramani, Phys. Rev. Lett. **77**, 55 (1996).
[28] M. V. Jacobson, Commun. Math. Phys. **81**, 39 (1981).
[29] C. Grebogi, E. Ott, and J. A. Yorke, Physica D **7**, 181 (1983).
[30] D. Gulick, *Directions in Chaos* (McGraw-Hill, New York, 1990).
[31] C. Grebogi, E. Ott, and J. A. Yorke, Phys. Rev. Lett. **50**, 935 (1983); Ergod. Theory Dyn. Syst. **5**, 341 (1985).
[32] C. Grebogi, S. W. McDonald, E. Ott, and J. A. Yorke, Phys. Lett. A **110**, 1 (1985).
[33] J. P. Eckmann and D. Ruelle, Rev. Mod. Phys. **57**, 617 (1985).
[34] C. Grebogi, E. Ott, and J. A. Yorke, Phys. Rev. A **37**, 1711 (1988).
[35] Y.-C. Lai, Y. Nagai, and C. Grebogi, Phys. Rev. Lett. **79**, 649 (1997).
[36] C. Grebogi, S. M. Hammel, J. A. Yorke, and T. Sauer, Phys. Rev. Lett. **65**, 1527 (1990).
[37] E. J. Kostelich, I. Kan, C. Grebogi, E. Ott, and J. A. Yorke, Physica D **109**, 81 (1997).

[38] R. S. Ellis, *Entropy, Large Deviations, and Statistical Mechanics* (Springer-Verlag, New York, 1985).

[39] M. G. Bulmer, *Principles of Statistics* (Dover, New York, 1979).

[40] W. Feller, *An Introduction to Probability Theory and Its Applications* (Wiley, New York, 1957), Vol. I.

[41] A. M. Batista, S. E. S. Pinto, R. L. Viana, and S. R. Lopes, Phys. Rev. E **65**, 056209 (2002).